Electronic Supplementary Material (ESI) for Polymer Chemistry.

Supporting Information for

Borinic Acid Block Copolymer: New Building Blocks for Supramolecular Assembly and Sensory Applications

Fei Cheng,[a]‡ *Wen-Ming Wan,*[a,b]‡* *Yan Zhou,*[b] *Xiao-Li Sun,*[c]
Edward M. Bonder,[d] *Frieder Jäkle*[a]*

[a] Department of Chemistry, Rutgers University Newark, 73 Warren Street, Newark, NJ 07102, United States.

[b] State Key Laboratory of Heavy Oil Processing and Centre for Bioengineering and Biotechnology, China University of Petroleum (East China), 66 Changjiang West Road, Qingdao Economic Development Zone, Qingdao, Shandong, 266580, People's Republic of China.

[c] Department of Material Physics and Chemistry, China University of Petroleum (East China), 66 Changjiang West Road, Qingdao Economic Development Zone, Qingdao, Shandong, 266580, People's Republic of China.

[d] Department of Biological Sciences, Rutgers University-Newark, 195 University Avenue, Newark, NJ 07102

‡ These authors contributed equally

* to whom correspondence should be addressed:

wanwenming@upc.edu.cn, fjaekle@rutgers.edu.

General Methods

The 499.9 MHz ^{1}H and 125.7 MHz ^{13}C NMR spectra were recorded on a Varian INOVA 500 MHz spectrometer. The 160.4 MHz ^{11}B NMR spectra were recorded with a boron-free probe using boron-free quartz NMR tubes. All NMR spectra were referenced internally to the solvent peaks.

GPC-RI analyses were performed in THF (1.0 mL/min, 35 °C) or DMF with 0.2% w/v of $[Bu_4N]Br$ (0.50 mL/min, 65 °C) using a Waters Empower system equipped with styragel columns, a 717plus autosampler, a 1525 binary HPLC pump, a 2487 dual λ absorbance detector, and a 2414 refractive index detector. Polystyrene standards (Polymer Laboratories, Varian Inc.) were used for calibration. Multi-angle laser light scattering (GPC-MALLS) experiments were performed at 690 nm (30 mW linear polarized GaAs laser) on a Wyatt Dawn EOS instrument in-line with the GPC, using the columns specified above. A Wyatt Optilab refractive index detector operated at 690 nm was used as the concentration detector and differential refractive indices dn/dc were calculated with the Wyatt Astra software assuming 100% mass recovery. The dynamic light scattering (DLS) measurement was performed at 25.0±1 °C with a Malver Zetasizer Nano-ZS instrument, equipped with a 4 mW, 633 nm He-Ne laser and an Avalanche photodiode detector at an angle of 173°.

UV-vis absorption data were acquired on a Varian Cary 500 UV-Vis / NIR spectrophotometer. Fluorescence data and quantum yields were measured on a Varian Cary Eclipse fluorescence spectrophotometer with optically dilute solutions ($A<0.1$). Anthracene was used as the standard and the quantum yield of anthracene (0.33 in THF) was adopted from the Handbook of Photochemistry. Sample solutions were prepared using a microbalance (±0.1 mg) and volumetric glassware. The quantum yields were calculated by plotting a graph of integrated fluorescence intensity vs. absorbance of at least 4 solutions with increasing concentration. The gradient of the graph is proportional to the quantum yield.

Transmission electron microscopy (TEM) was conducted on a FEI Tecnai 12 electron microscope operated at 80 kV. One drop of polymer aggregates solution was cast on a copper grid with a carbon coating.

AFM measurements were performed with a Nanoscope VIII MultiMode AFM (Digital Instruments, Bruker, USA) in tapping mode. Topographic images were concurrently recorded under ambient conditions, at 512 × 512 pixel resolution and a scanning speed of 1 Hz.

Electrochemical experiments were carried out with a CHI 660D electrochemical workstation (ChenHua, Shanghai) in a standard three-electrode cell consisting of a glassy carbon electrode with a diameter of 3 mm as the working electrode, a saturated calomel electrode (SCE) as the reference electrode, a Pt wire counter electrode, and PBS buffer (0.1 M, pH = 7.0) as the electrolyte.

Supporting Data

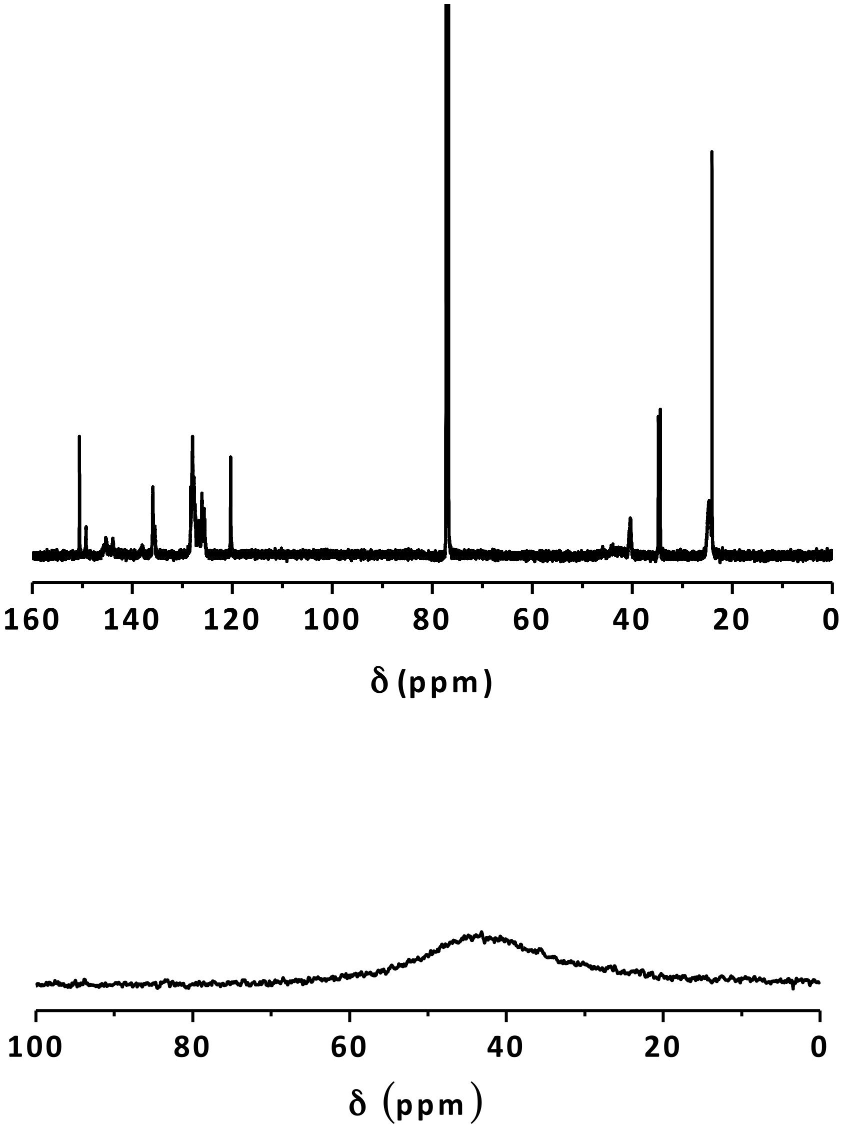

Figure S1. ^{13}C and ^{11}B NMR spectra of PS-*b*-PBA in $CDCl_3$ (^{1}H NMR spectrum is given in the main text)

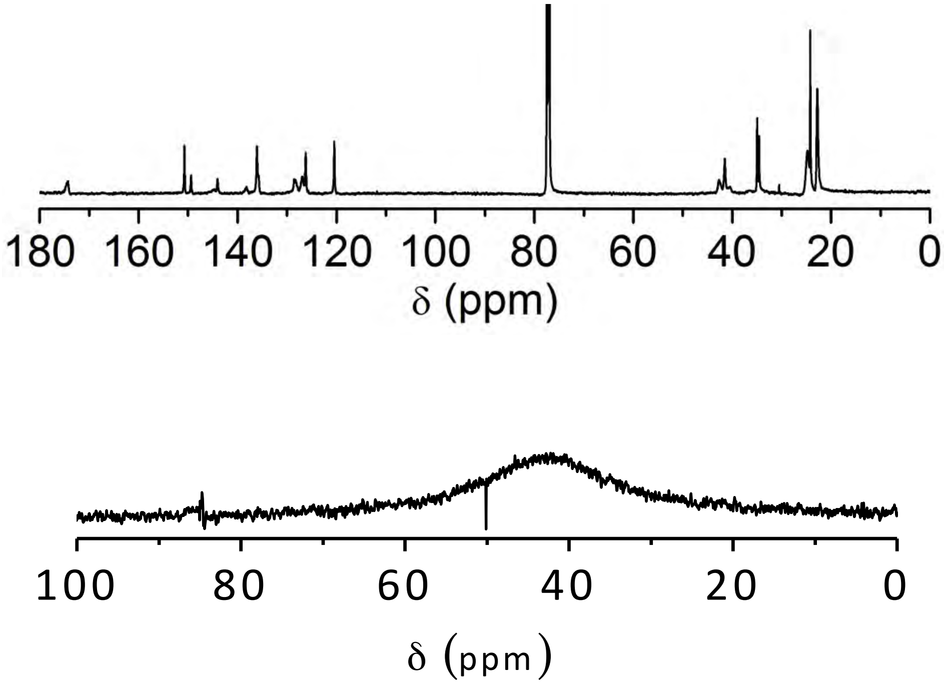

Figure S2. ^{13}C and ^{11}B NMR spectra of PNIPAM-*b*-PBA in $CDCl_3$ (^{1}H NMR spectrum is given in the main text)

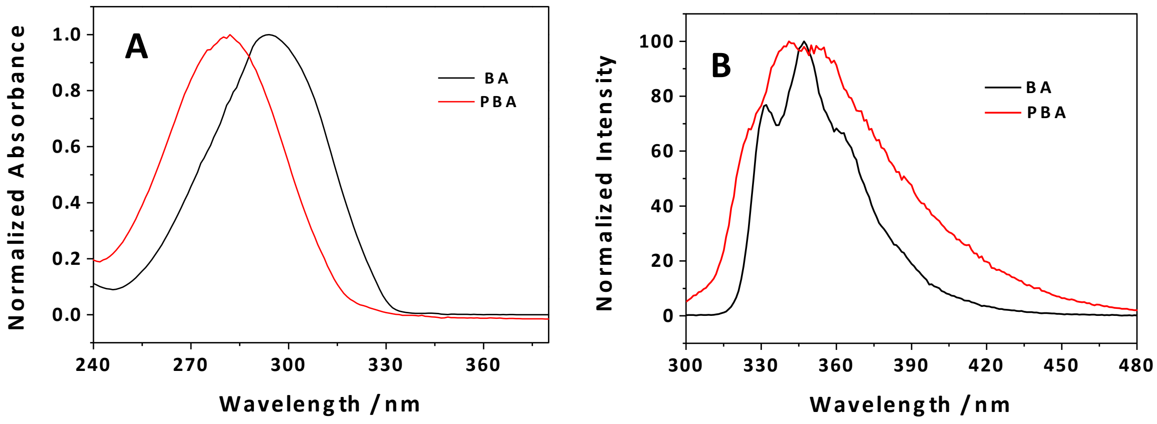

Figure S3. Absorption (left) and emission (right) spectra of PBA (red) and BA (black) in THF.

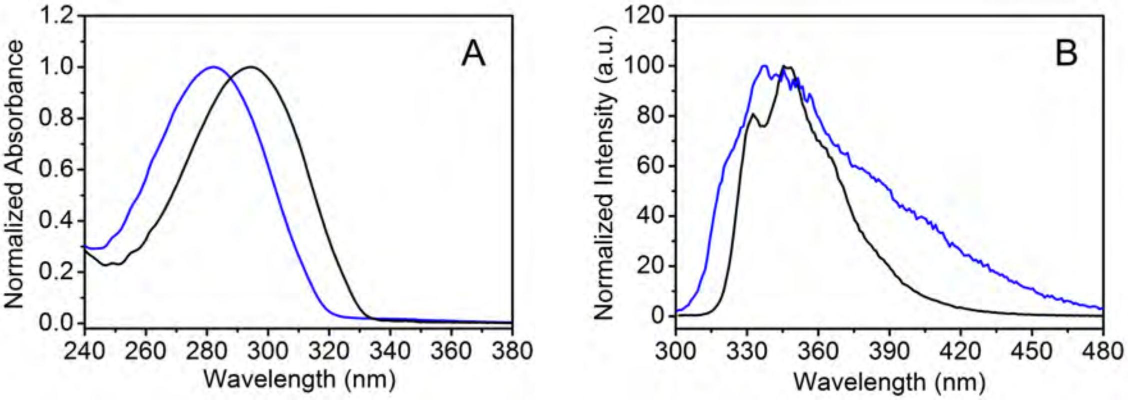

Figure S4. Absorption (left) and emission (right) spectra of PS-*b*-PBA (blue) and BA (black) in THF.

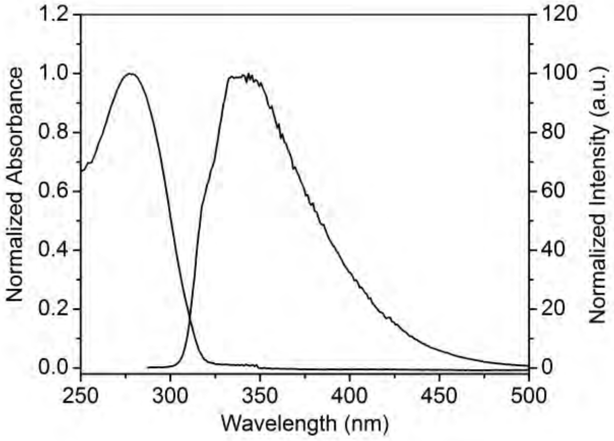

Figure S5. Absorption and emission spectra of PNIPAM-*b*-PBA in THF.

H-bonding induced supramolecular co-assembly of PS-*b*-PBA/P4VP. To a solution of PS-*b*-PBA (3.0 mg) in 5.0 mL of chloroform, was added a solution of 0.5 mg P4VP homopolymer in 1.0 mL of chloroform under stirring. The as-formed solution was used for characterization.

H-bonding induced supramolecular co-assembly of PNIPAM-*b*-PBA/P4VP. To a solution of PNIPAM-*b*-PBA (3.0 mg) in 5.0 mL of chloroform, was added a solution of 0.5 mg P4VP homopolymer in 1.0 mL of chloroform under stirring. The as-formed solution was used for characterization.

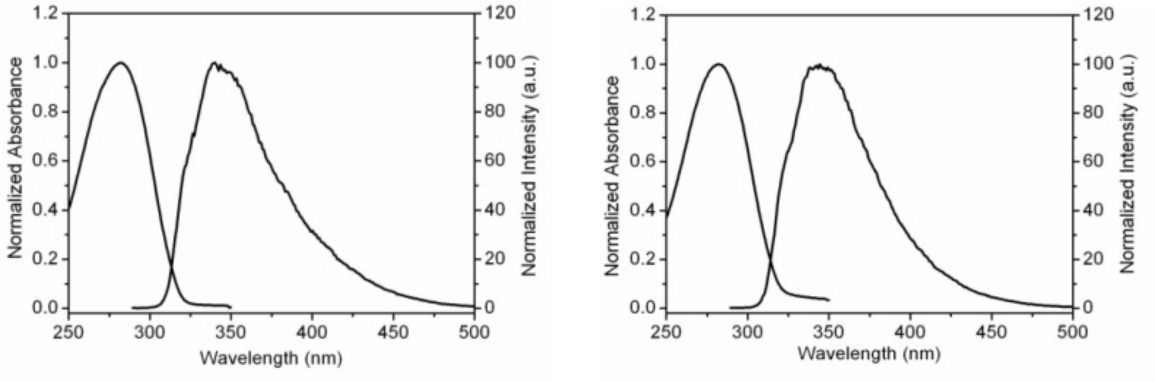

Figure S6. Absorption and emission spectra of (left) PS-*b*-PBA/P4VP and (right) PNIPAM-*b*-PBA/P4VP solutions in chloroform.

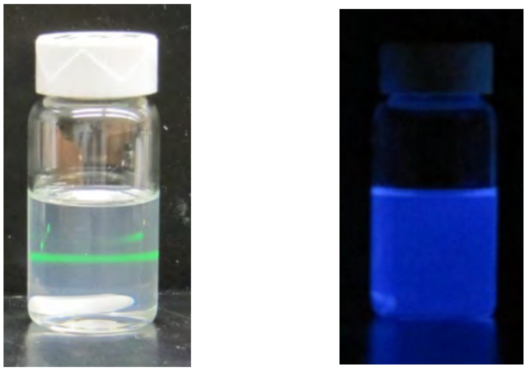

Figure S7. Representative photographs of PNIPAM-*b*-PBA/P4VP supramolecular aggregate solutions in chloroform. (left) Solution with a green laser beam illustrating lights scattering due to aggregate formation; (right) under irradiation with a hand-held UV lamp.

NMR evidence of an H-bonding interaction between borinic acid monomer BA and pyridyl compounds. To a solution of the borinic acid monomer BA (~10 mg) in 0.5 mL of $CDCl_3$, was added a drop of 4-^{t}butylpyridine and the ^1H NMR spectrum was recorded. An H-bonding interaction between the borinic acid and pyridyl group is suggested by the disappearance of the B-OH signal at 5.82 ppm (the signal is possibly shifted to a region where it overlaps with another signal). The ^{11}B NMR spectrum of this mixture is identical to that of the borinic acid monomer itself.

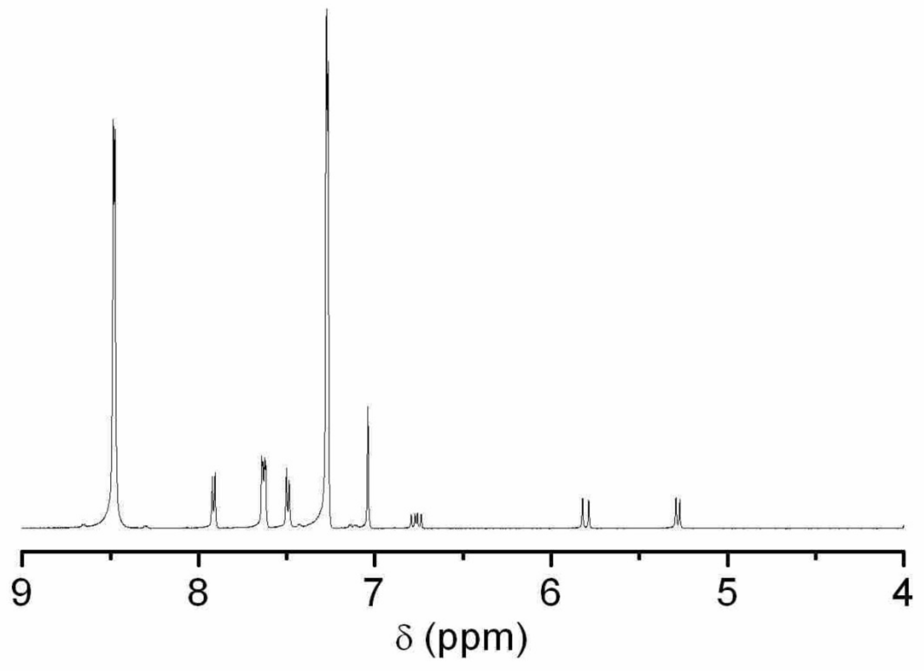

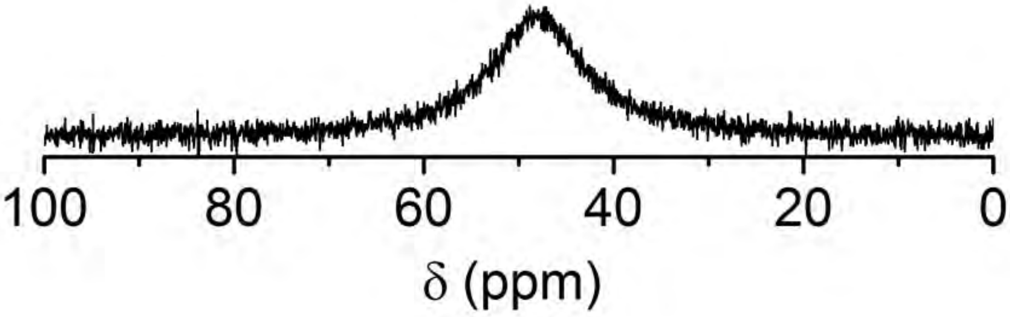

Figure S8. ^1H and ^{11}B NMR spectra of BA monomer/4-^{t}Bu pyridine mixture in $CDCl_3$

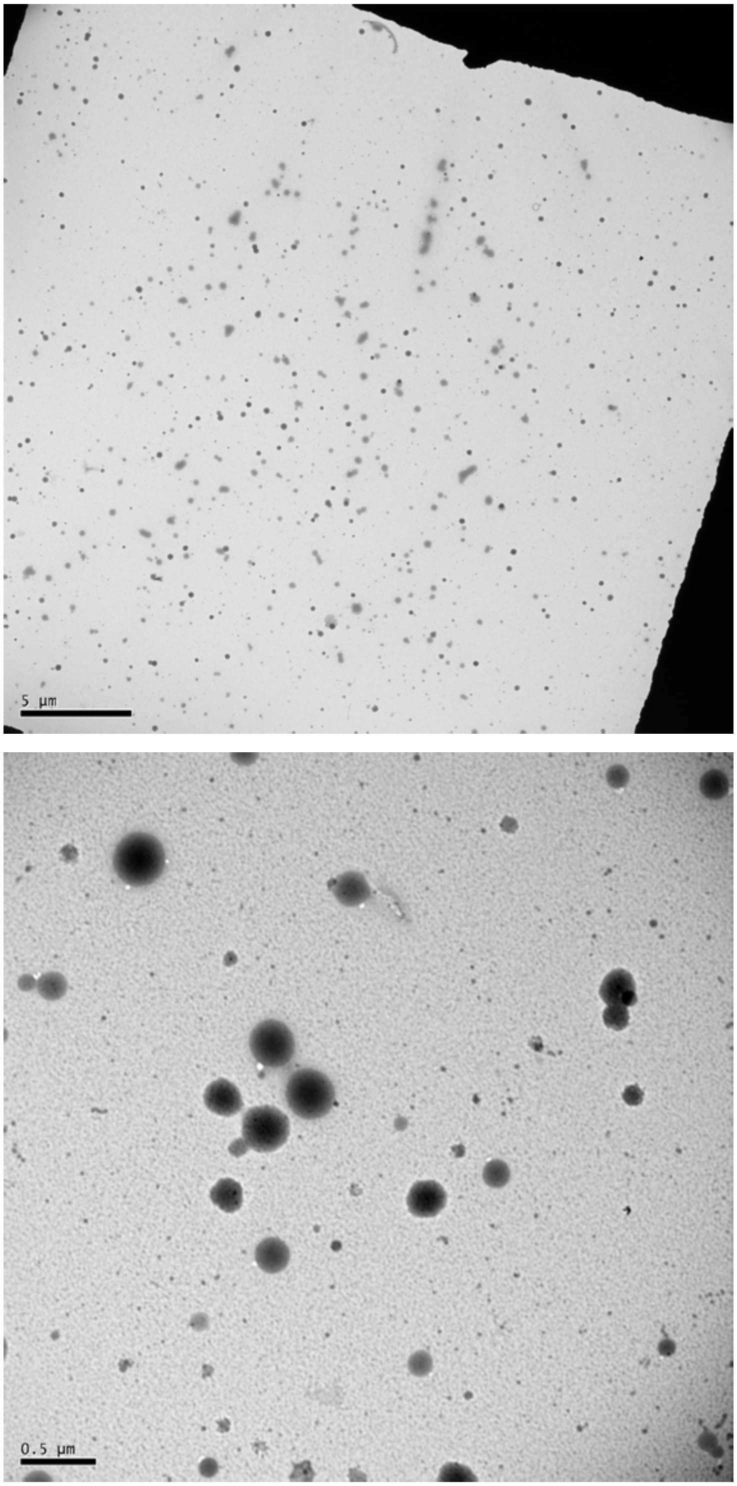

Figure S9. TEM images of PNIPAM-*b*-PBA/P4VP supramolecular aggregates.

F⁻ anion binding to borinic acid monomer. To a quartz NMR tube containing a solution of 5.0 mg of BA in 0.5 mL of THF, predetermined amounts of TBAF (1.0 M) in THF were added. ^{11}B NMR was used to monitor the binding process at different stoichiometric ratios of F⁻/borane. APCI mass spectrometry was used to identify the structure of the final product.

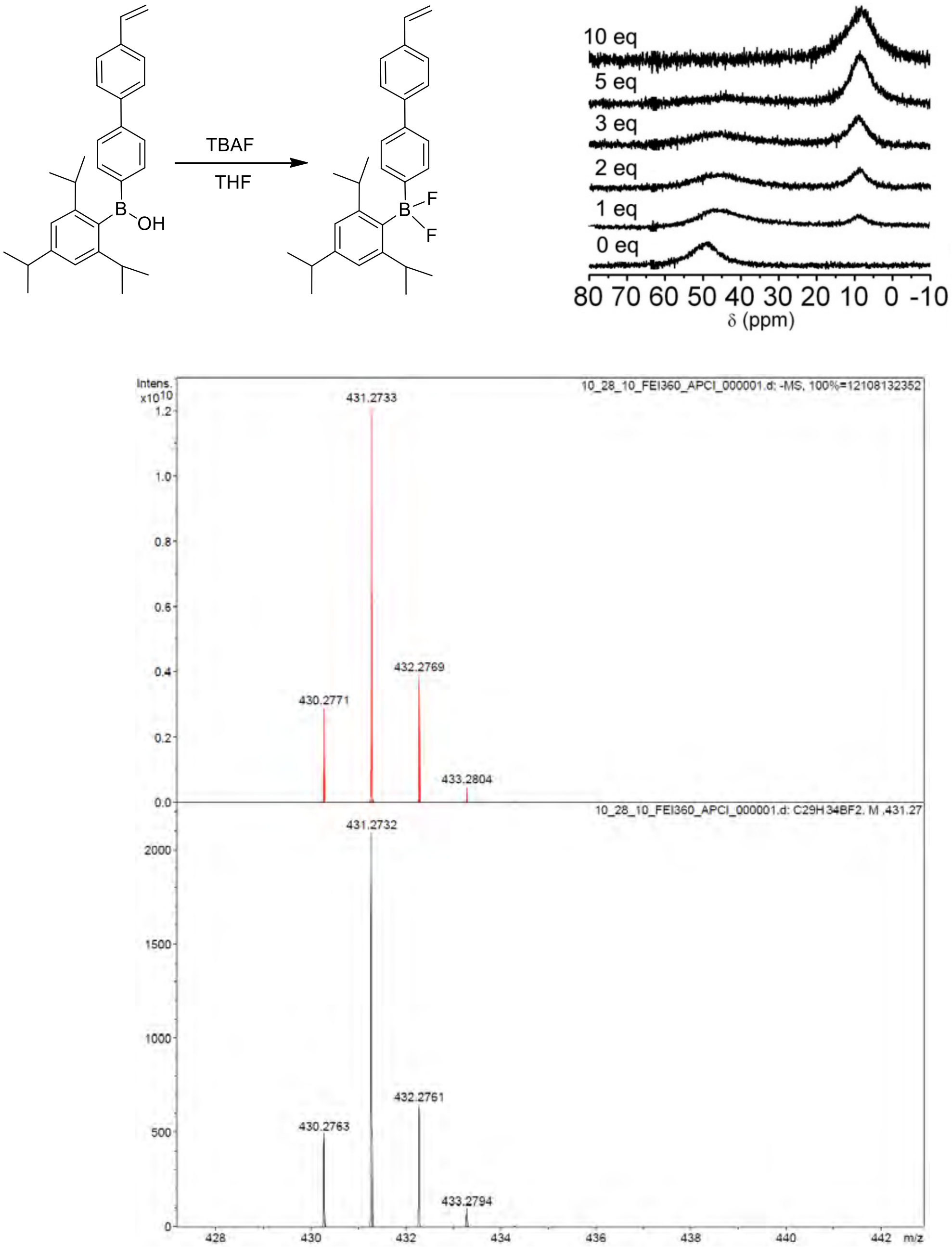

Figure S10. (top) ^{11}B NMR spectra of BA/F⁻ complex in THF; (bottom) MALDI-MS spectrum of borinic acid monomer/F⁻ (molar ration of F⁻/B = 10/1) complex

Reactivity of borinic acid model compound with methanol. The borinic acid model compound iodophenyl(triisopropylphenyl)borinic acid and methanol were mixed in a ratio of 1:1 for 10 mins at room temperature. The product was obtained upon removal of all volatile components under high vacuum.

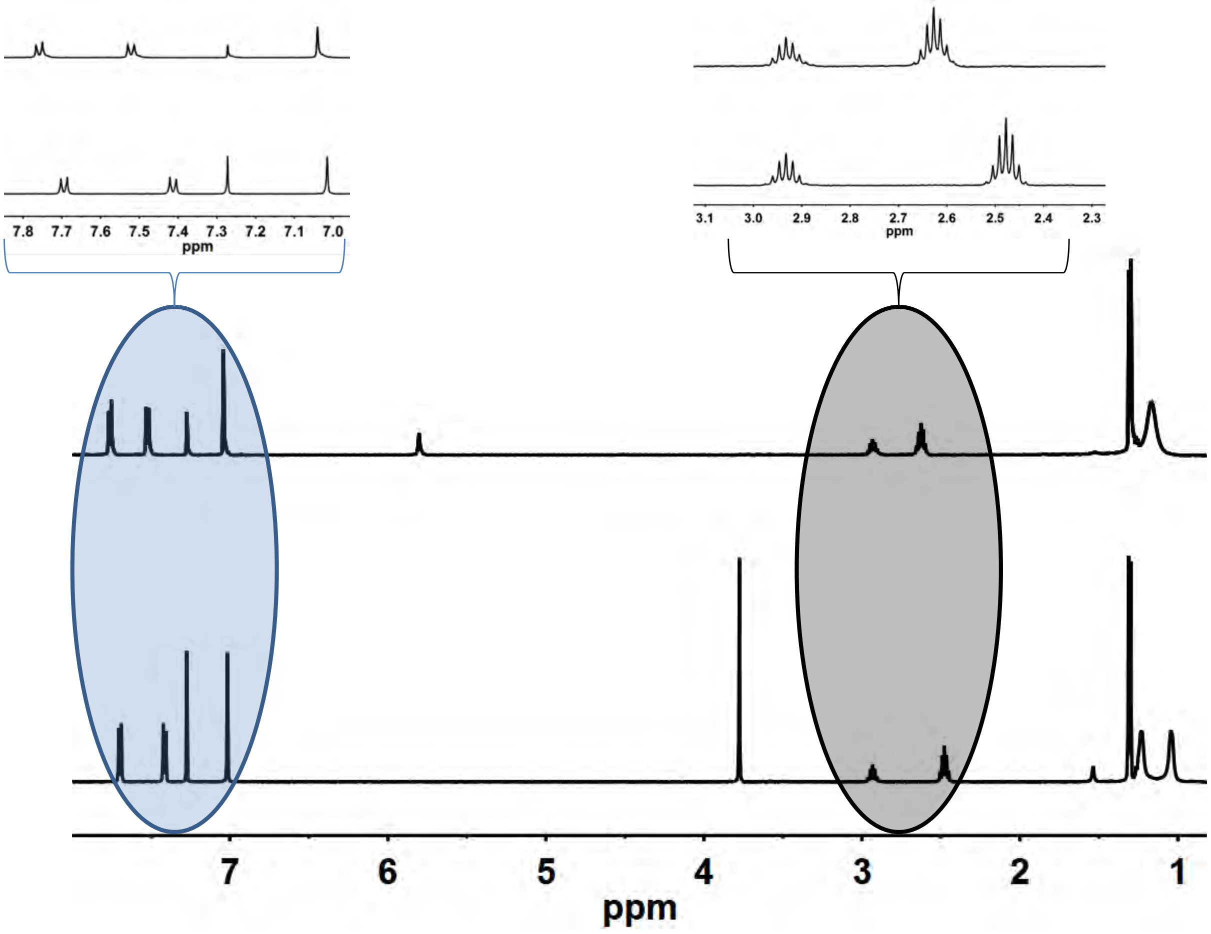

Figure S11. ^{1}H NMR spectra of iodophenyl(triisopropylphenyl)borinic acid before (top) and after (bottom) reaction with methanol.

Reactivity of borinic acid model compound with ethylene glycol. The borinic acid model compound iodophenyl(triisopropylphenyl)borinic acid and ethylene glycol were mixed in a ratio of 2:1 for 10 mins at room temperature, followed by MALDI-MS characterization (anthracene matrix).

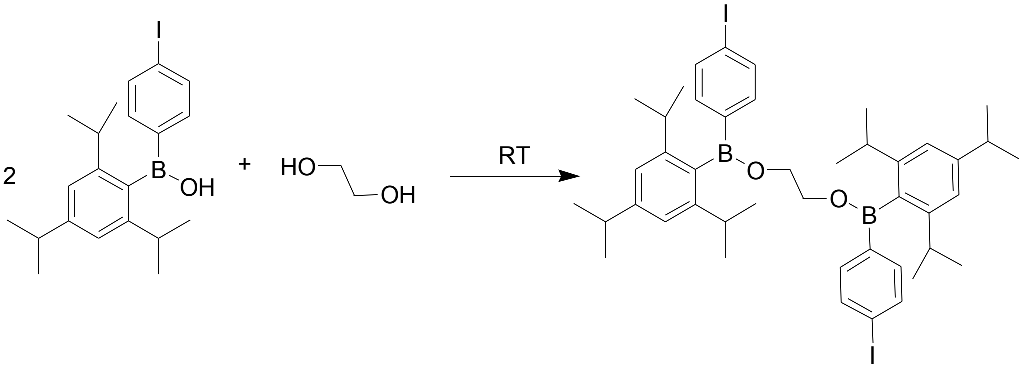

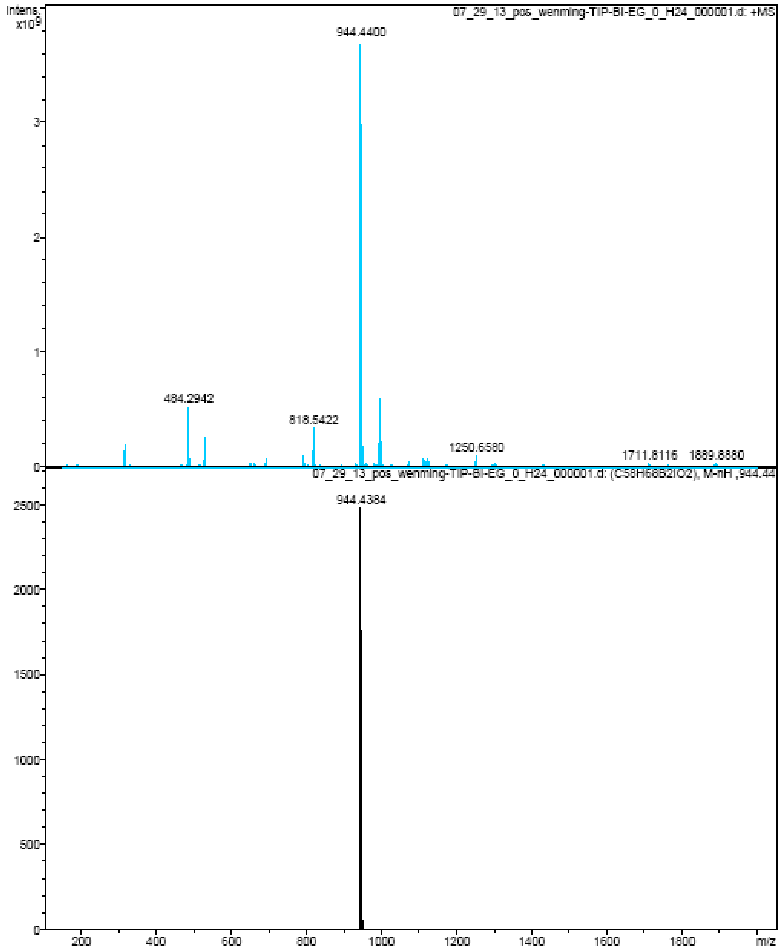

Figure S12a. MALDI-MS spectra of the product from reaction of borinic acid model compound and ethylene glycol

Expansion for (M^+ –I + anthracene) peak, $C_{58}H_{68}B_2IO_2$

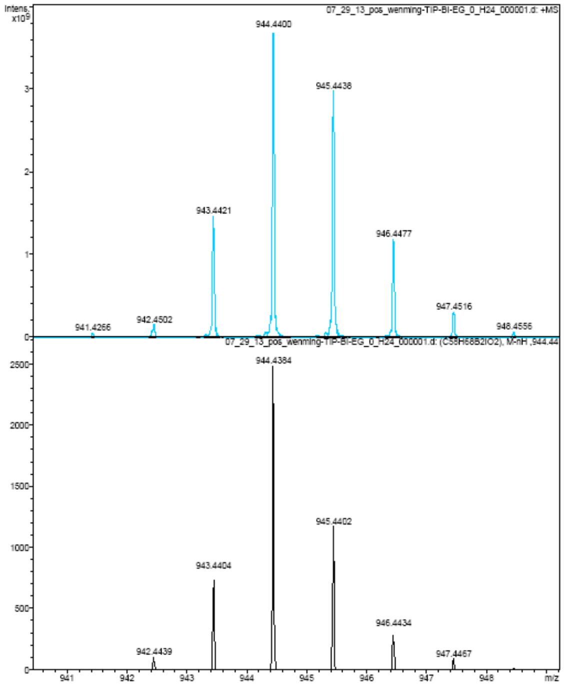

Expansion for (M^+ –2I + 2anthracene) peak, $C_{72}H_{78}B_2O_2$

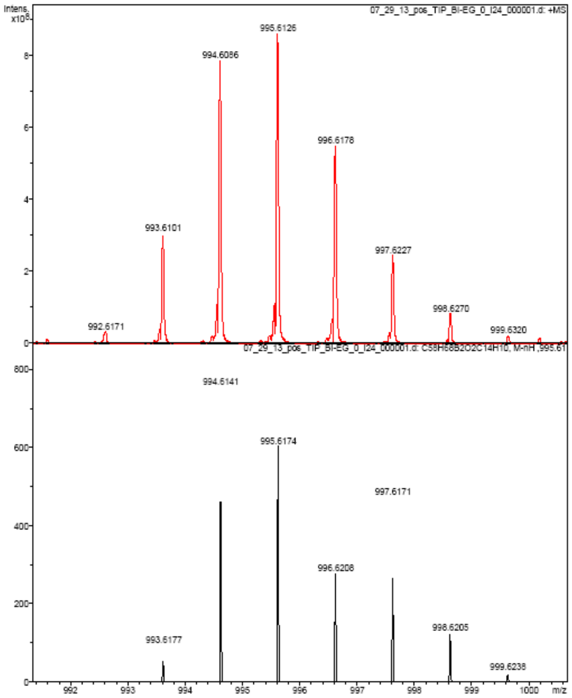

Figure S12b. Expansions of MALDI-MS spectra of the product from reaction of borinic acid model compound and ethylene glycol.

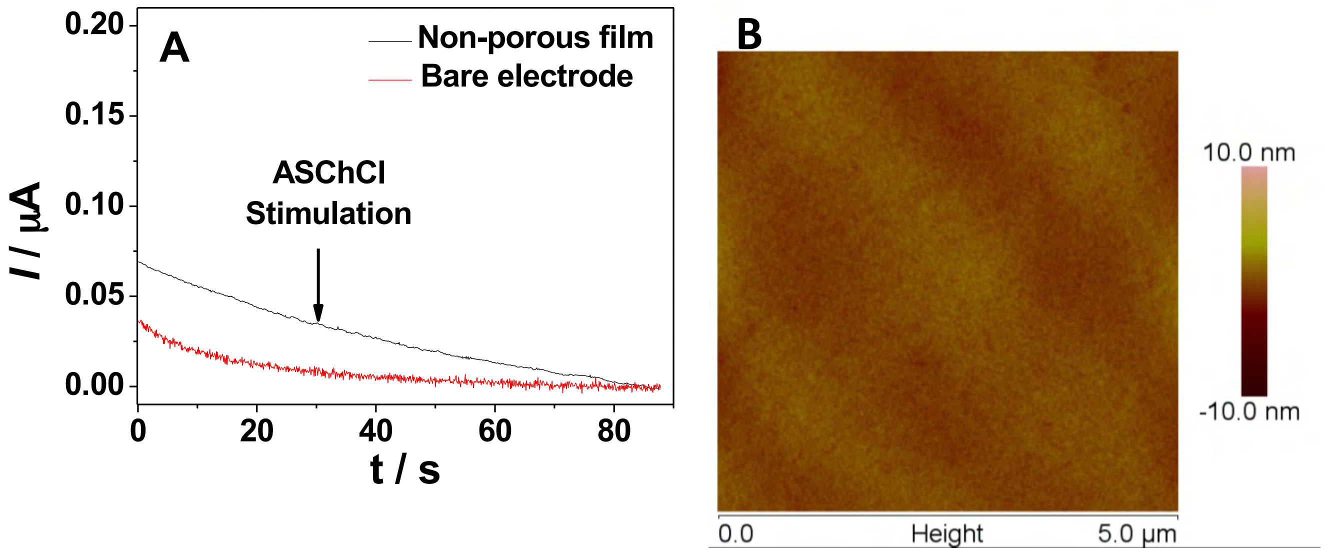

Figure S13 A). Current-time curves for ASChCl stimulation in control experiments with the bare, uncoated electrode (red line) and with a non-porous, continuous film (black line). B) AFM image (height) of PS-*b*-PBA block copolymer film cast on mica from anhydrous THF ([PS-b-PBA] = 1 mg/mL).